



Promoting effect of nitration modification on activated carbon in the catalytic ozonation of oxalic acid

Hongbin Cao ^{a,b,c}, Linlin Xing ^{a,b,c}, Guangguo Wu ^{a,b,c}, Yongbing Xie ^{a,b,c,*}, Shaoyuan Shi ^{a,b,c}, Yi Zhang ^{a,b,c}, Daisuke Minakata ^d, John C. Crittenden ^{d,1}

^a Key Laboratory of Green Process and Engineering, Institute of Process Engineering, Chinese Academy of Sciences, Beijing 100190, China

^b Research Centre for Process Pollution Control, Institute of Process Engineering, Chinese Academy of Sciences, Beijing 100190, China

^c National Engineering Laboratory for Hydrometallurgical Cleaner Production Technology, Beijing 100190, China

^d Brook Byers Institute for Sustainable Systems, Georgia Institute of Technology, Atlanta, GA 30332, United States



ARTICLE INFO

Article history:

Received 30 October 2012

Received in revised form 5 May 2013

Accepted 7 May 2013

Available online 21 May 2013

Keywords:

Catalytic ozonation

Activated carbon

Surface modification

Nitration

Amination

ABSTRACT

A commercial activated carbon (AC) was modified with a nitration or amination method, and the effects of textural and chemical properties on the ability of the AC samples to destroy oxalic acid (OA) using ozone was investigated in this work. The degradation rates of OA on the nitrated and aminated AC samples increased by 38.5% and 9.6%, respectively. The adsorption capacity of the AC sample was not enhanced after modification, but the decomposition rate of ozone in solution increased. The surface area of AC significantly decreased after nitration because the entrance of micropores and some larger pores were blocked by the modified functional groups. In addition, the surface area was recovered when the nitrated AC was further aminated. We demonstrated that the enhancement in the catalytic activity was primarily caused by the differences in surface chemistry. The pH_{pzc} values and Boehm titration results showed that nitration increased the acidity of the AC, while more basic groups were grafted after amination. X-ray photoelectron spectroscopy (XPS) and temperature programmed desorption (TPD) results confirmed that –NO₂ and acid oxygenated groups were simultaneously grafted onto AC during nitration. Meanwhile, the –NO₂ group was completely reduced to –NH₂ and the carboxylic groups were partially reduced during amination. The basic groups (–NH₂ and possible pyrone groups) enhanced the catalytic activity of the aminated AC sample, and the increased activity of the nitrated AC material was mainly due to the acid oxygenated surface groups.

© 2013 Elsevier B.V. All rights reserved.

1. Introduction

Water in China is suffering from severe pollution of heavy metal ions, chemical oxygen demand (COD), ammonia nitrogen, petroleum, toxic organic compounds, refractory organic compounds, etc. Among them, refractory organic compounds are particularly harmful because of their easy enrichment into fauna and flora, as well as their carcinogenesis, teratogenesis and mutagenesis effects. Advanced oxidation processes (AOPs) have attracted great interest in the past two decades because of their high efficiency in refractory organics removal, especially catalytic

ozonation [1–5]. Ozone can easily react with unsaturated aromatic and aliphatic compounds, but it has a low reaction rate with saturated organic compounds. This property restricts its application in chemical oxidation. With the aid of homogeneous or heterogeneous catalysts, a higher number of hydroxyl radicals ($\cdot\text{OH}$) are produced from ozone decomposition. The production of $\cdot\text{OH}$ from ozone is responsible for the effectiveness of ozone in destroying organic compounds because $\cdot\text{OH}$ is a strong oxidant that unselectively reacts with electron-rich organics. Carbon materials have been widely studied in heterogeneous catalytic ozonation, because of their wide availability, as well as various pore sizes, surface areas and surface chemistries [6,7]. A work has recently shown that a larger surface area benefits catalytic ozonation [8]. However, the effects of surface functional groups on catalytic activity have not yet been fully revealed.

Surface modification procedures that enhance catalytic ozonation are widely investigated. These procedures include heat treatment under different atmospheres, ozone, H₂O₂ and HNO₃ treatments, as well as nitrogenation and sulfuration treatments

* Corresponding author at: Key Laboratory of Green Process and Engineering and Research Centre for Process Pollution Control, Institute of Process Engineering, Chinese Academy of Sciences, Beijing 100190, China. Tel.: +86 01082544844.

E-mail addresses: ybxei@home.ipe.ac.cn (Y. Xie), john.crittenden@ce.gatech.edu (J.C. Crittenden).

¹ Tel.: +1 404 894 7895.

[7]. In these procedures, surface functional groups and pore size distribution varied accordingly, thereby affecting the adsorption capacity and catalytic activity. However, no consensus has been reached on the effects of surface functional groups, pore size distribution and internal/external surface areas with respect to the performance in the catalytic ozonation.

In most of the published papers, it was recognized that basic groups were favorable to catalytic ozonation. Sánchez-Polo et al. [8] found that carbons with high basicity and large surface areas were the most active catalyst for catalytic ozonation. They found that the interaction between ozone and pyrrol groups generates a higher number of $O_2\cdot-$, which in turn generates more $\cdot OH$ from ozone [8]. Liu [9] modified carbon nanotubes (CNTs) with different heat treatments and related their activities with acidities. The Boehm titration results clearly indicated a reduction in acid groups and an increase in the number of basic groups on the modified CNTs, which show significantly increased activity in oxalic acid (OA) removal. Activated carbon (AC) with high basicity favors ozone decomposition [10]. The loss of activity of AC during use is possibly due to the decrease in basic groups as well as the increase in acid groups [2,11].

However, acidic surface groups also play a positive role in the interaction between AC and O_3 . Chedeville [12] found that ACs with lower external surfaces, equivalent numbers of basic functions and more acid functions was more active than other AC samples. It was suggested that both acidic and basic functional groups may favor $\cdot OH$ generation in the catalytic ozonation of diethyl phthalate [13]. These different conclusions indicate that the effects of surface groups of carbon materials on catalytic ozonation still require further investigation. Meanwhile, most studies on AC catalytic ozonation only discuss the oxygenated groups on the surface. Nitrogen modification on AC surfaces has been investigated in many works, but the effect of this modification on AC catalytic ozonation remains undetermined.

In this work, the $-NO_2$ group was added to a commercial AC during nitration modification, and was then converted to $-NH_2$ in subsequent amination step. Apart from the nitrogen containing groups, various oxygenated surface groups were also grafted. The textural and chemical properties, as well as the activities of the resulting ACs in the catalytic ozonation of OA before and after surface modification, were compared. By excluding the influence of surface area, ash content and adsorption capacity, the relationship between surface functional groups and the catalytic activities of modified ACs was determined.

2. Experimental

2.1. Modification of AC samples

AC was purchased from Sigma Aldrich (100–400 mesh, untreated powder). The AC was pretreated with a solution of 15% HCl and 5% HF. The suspension was then stirred for 24 h at 293 K before use, to remove ash and eliminate its impact on catalytic ozonation. After filtration, the AC sample was washed with ultra-pure water until the pH of the filtrate was nearly neutral. The sample was then dried at 393 K for 12 h. The obtained sample was named AC-A to indicate that it was acid washed.

Nitration modification of the AC-A sample was performed according to a previously reported method [14]. Thirty milliliters of fuming nitric acid was slowly dripped into a suspension of 1 g of AC-A and 40 ml of acetic anhydride in a 1000 ml three-necked flask at 273 K. After stirring at this temperature for 5 h and subsequently stirring for 19 h at 293 K, the solid sample was filtrated and washed until the filtrate was neutral. The sample was dried at 378 K for 12 h, and labeled AC- NO_2 .

Amination of the AC- NO_2 sample was conducted as follows. One gram of AC- NO_2 was mixed with 10 ml of strong aqua ammonia and 20 ml of pure water. After adding 0.75 g of sodium borohydride, the suspension was kept at 293 K for 24 h under stirring. The solid was filtrated, washed until the filtrate was neutral, and then dried at 378 K for 12 h. The obtained sample was labeled AC- NH_2 .

2.2. Characterization of AC samples

Surface area, pore size distribution, and surface properties are the key factors affecting the catalytic performance of ACs. The pore structures and surface areas of the AC samples were determined by nitrogen adsorption, which was performed on a physical adsorption instrument (Autosorb-iQ, Quantachrome). The samples were degassed at 423 K for 12 h. Nitrogen adsorption and desorption isotherms were then obtained at 77 K. NLDFT, the *t*-plot method and BET model were used to calculate the pore size distribution, pore volume and surface area, respectively.

Boehm titration, Fourier transform infrared spectroscopy (FTIR), temperature programmed desorption (TPD), and X-ray photoelectron spectroscopy (XPS) were conducted to verify the surface functional groups on the AC samples. The amount of basic surface groups was determined by titration with 0.01 M of HCl solution. A mixture of 0.5 g of AC samples and 25 ml of HCl solution was shaken for 24 h at 298 K. The AC samples were then filtrated and carefully washed. All filtrates were collected and subsequently diluted to 100 ml. Using Phenolphthalein as indicator, about 100 ml of filtrate was then titrated with 0.01 M NaOH solution. The number of basic functional groups was then calculated as follows:

$$Q(\text{mmol/g}) = C_{\text{HCl}} \times (25 - C_{\text{NaOH}} \times V_{\text{NaOH}}/C_{\text{HCl}})$$

FTIR spectra were obtained using a spectrophotometer (Spectrum GX, PerkinElmer) within the measurement range of 15,000–2 cm^{-1} . A small amount of dried AC samples and 0.15 g of KBr were thoroughly mixed and then pressed under 20 MPa for 5 min to prepare the wafer for analysis. TPD was performed on a simultaneous thermal analyzer (STA-449, Netzsch) connected to an FTIR spectrometer (EQUINOX 55, Bruker). The samples were heated up to 1323 K at a rate of 20 K/min under a helium flow. The signals of the released CO and CO_2 during heating were then recorded. XPS analysis was performed on an X-ray photoelectron spectroscopy (ESCALAB 250Xi, Thermo Scientific Ltd) at an energy resolution $\leq 0.45 \text{ eV}$. The surface composition and binding energies profiles of carbon, oxygen, and nitrogen were then recorded.

The pH of point of zero charge (pH_{pzc}) was measured by the pH drift method [15]. Twenty-five milliliters of a 0.01 M NaCl solution was placed in a conical flask. The initial pH of the solution was adjusted within a wide range using 0.1 M HCl and 0.1 M NaOH solution. After adding 0.15 g of AC samples, the suspension was stirred for 3 h at a rate of 200 rpm under a nitrogen atmosphere at 298 K. The final pH was plotted against the initial pH, and the pH_{pzc} was obtained at the point when $pH_{\text{initial}} = pH_{\text{final}}$.

2.3. Catalytic ozonation of OA

The reaction was performed in a 500 ml semi batch reactor. The initial concentration of OA in the reaction solution was about 50 mg/L, and the corresponding pH of solution was about 3. A neutral solution adjusted using 0.01 M NaOH solution was also prepared for comparison. Ozone was produced by an ozone generator (COM-AD-01, Anseros) from pure oxygen at a flow rate of 150 cm^3/min . The ozone in the inlet gas was kept at 50 mg/dm 3 , and the dosage of the AC sample was 0.2 g/L. The solution in the reactor was strongly stirred. Samples were obtained after certain intervals and analyzed on an ion chromatograph (IC, DX500, Dionex). The eluent was 0.05 mol/L of NaOH solution with a flow rate of 1 ml/min. The ozone concentration in the inlet and outlet gas was monitored

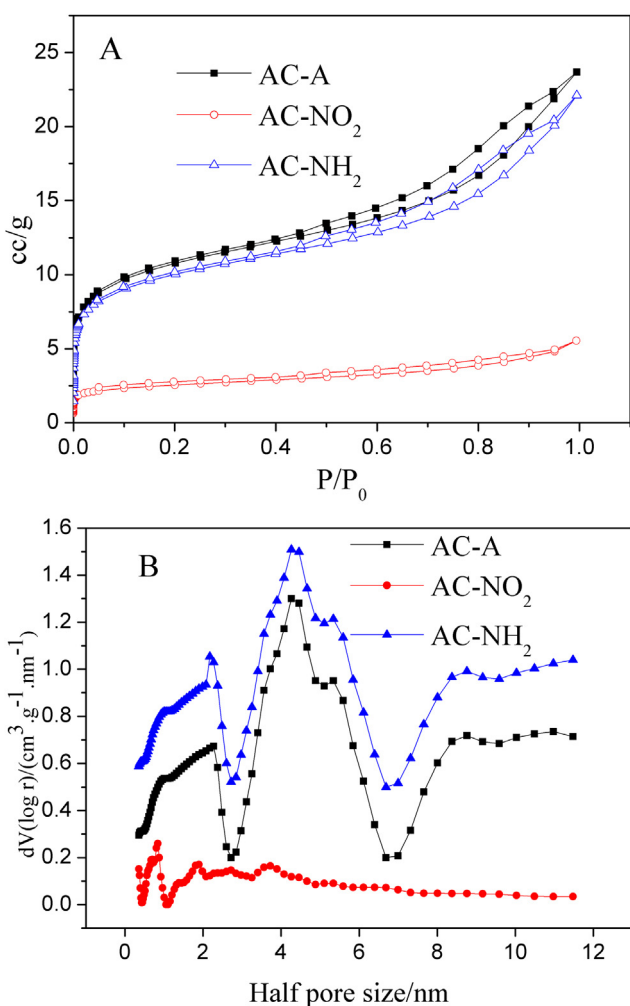


Fig. 1. Physical adsorption isotherms (A) and pore size distributions (B) of the AC samples.

by an ozone analyzer (OzomatGM-PRO, Anseros). The ozone concentration in the solution was analyzed by the indigo method. The inorganic carbon (IC) in the solution was also examined with a total organic carbon analyzer (TOC-V CPH, Shimadzu).

3. Results and discussion

3.1. Textural and chemical characterization of AC samples

The commercial AC was first treated with an acid solution to remove ash content. Trace amounts of Mg, Fe, Al, Co, Mn, Mo and Ti were washed out and the total loss in weight percent was $\leq 1.2\%$. The surface area of AC-A slightly increased from 1061 to 1128 m²/g after acid pretreatment.

Fig. 1 shows the physical adsorption results of the AC samples before and after surface modification. The physical adsorption/desorption isotherms at 77 K were obtained to calculate the surface area and pore volumes of AC samples, and the results are shown in Fig. 1(A). The BET surface areas for AC-A, AC-NO₂ and AC-NH₂ were 1128, 232 and 1023 m²/g, respectively. This indicated a significant decrease in surface area after nitration. However, this loss was recovered after amination, different from that reported by Chingombe [16,17] who reported a slight increase in surface area after a similar surface modification with $-\text{NO}_2$ groups. Our finding was consistent with that in the review article of Rivera-Utrilla et al. [7], who found that the surface area of carbon materials changes

Table 1
Physical properties of different AC samples.

| Samples | Total surface area (m ² /g) | External surface area (m ² /g) | Micropore volume (cm ³ /g) |
|--------------------|--|---|---------------------------------------|
| AC-A | 1128 | 496 | 0.269 |
| AC-NO ₂ | 232 | 100 | 0.055 |
| AC-NH ₂ | 1023 | 409 | 0.263 |

after various modifications, depending on the reaction condition and the type of carbon material. They found that the BET surface area of some AC samples markedly decreased after treatment in a boiling solution of HNO₃ or under severely acid conditions for a long time. Pore wall destruction and internal surface area decrease possibly happened on AC samples during these processes [18,19]. Oxygen surface complexes fixed at the entrance of micropores could also cause the decrease in nitrogen adsorption capacity [19,20]. In the current study, the surface area was recovered after amination. Therefore, it is reasonable to postulate that the decrease of surface area of AC-NO₂ was caused by the occupation of functional groups on the entrance of micropores of AC samples, and not by micropore collapse. These groups were subsequently removed or modified during the amination step, and the surface area was recovered.

Table 1 lists all parameters such as the total and external surface area, as well as the micropore volumes of the three AC samples. AC-A and AC-NH₂ showed highly similar structures, while AC-NO₂ was markedly different. The total and external surface areas and the micropore volume all decreased. This result indicated that the entrances of micropores were occupied during nitration modification, and that some larger pores were partly filled. This finding was consistent with that shown in Fig. 1(B).

Basic functional groups are generally considered as active sites for catalytic ozonation. In this study, the amount of these groups on AC samples was determined by titration with HCl solution. The amount changed from 234.8 to 186.2 and 764.5 mmol/g after nitration and amination treatments, respectively. This was confirmed by the corresponding pH_{pzc} values obtained with Boehm titration method. A higher number of basic functional groups increased the pH_{pzc} value, and vice versa. The pH_{pzc} of AC-NO₂ decreased from 2.6 to 1.8, whereas that of AC-NH₂ increased to 7.0. These changing trends were consistent with those reported in the literature [16,17].

The desorption signals of CO and CO₂ from the different AC samples during temperature programmed heating are displayed in Fig. 2. Generally, CO comes from the decomposition of weakly acid groups. AC-NO₂ showed a very strong CO peak with 723–973 K, which indicated the existence of lactone, phenol and anhydride groups on the surface [21]. The peak intensities of these groups on AC-NH₂ were much lower within the same temperature range. A strong CO peak at 1223 K was exhibited by AC-NH₂. This result may be due to pyrone groups, and this can partly explain the basicity of AC-NH₂ sample [22]. The CO peak at around 500 K on AC-NO₂ may be due to the condensation of two adjunct carboxylic groups [23,24].

Anhydrides and lactones were reported to evolve a mixture of CO and CO₂ [24], which are found in Fig. 2(A) and (B). AC-NO₂ showed three obvious peaks at around 573, 823 and 1233 K. These peaks were characteristic of carboxylic groups, lactones and anhydrides, and pyrones, respectively. The peak at around 573 K on AC-NH₂ almost completely disappeared, indicating that a significant amount of carboxylic acid was created on the surface after nitration, and subsequently eliminated after amination. The shoulder peak from 773 to 873 K on AC-NO₂, corresponding to lactones and anhydrides, was also more intense than that on the other two samples. These acid groups particularly carboxylic acid lowered the pH_{pzc} of AC-NO₂.

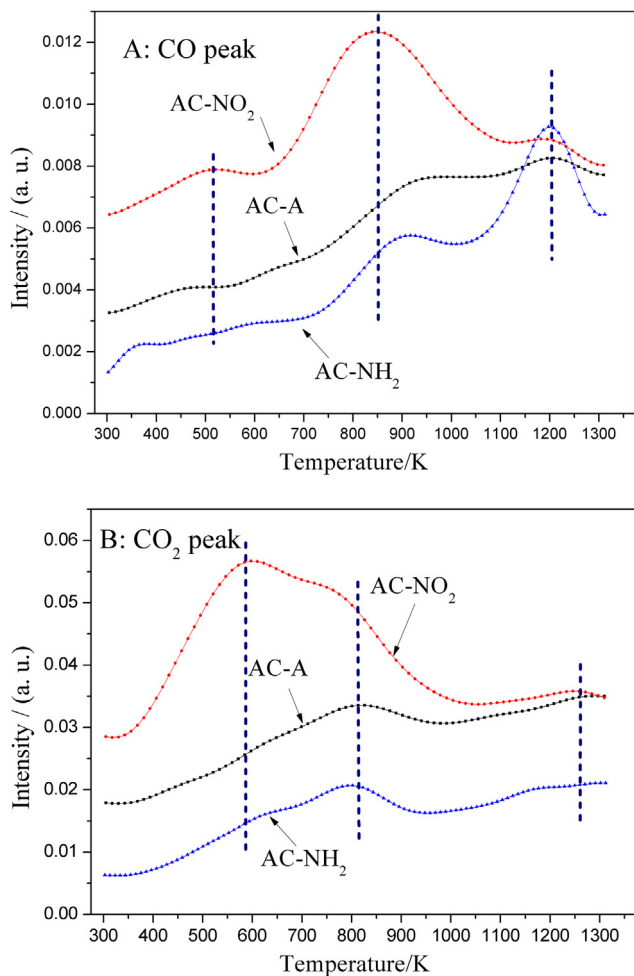


Fig. 2. TPD of the acid treated and surface modified AC samples (A: CO peaks, B: CO₂ peaks).

The TPD results show that a large amount of oxygenated groups was formed on the surface of AC-NO₂, and pyrone groups were formed on the AC-NH₂ surface, consistent with the previously reported one [16]. XPS analysis was further conducted to determine the surface element composition and binding energies of individual components. Table 2 shows the atomic ratios of the main elements on the surfaces of AC samples.

Only a trace amount of nitrogen was detected on AC-A, which was possibly originated from weekly physisorbed nitrogen impurities on the surface [25]. The nitrogen content on AC-NO₂ increased by 3.3%, which indicated that nitrogen containing functional groups such as -NO₂ were grafted onto the surface [14]. The amount of oxygen also increased, consistent with the TPD results indicating that a large number of oxygen containing groups were modified on the surface. After reduction by NaBH₄ in the amination step, the content of oxygen on the surface decreased from 23.1% to 18.7%. This result implied that some oxygenated functional groups were reduced. Detailed analysis indicated that -(C=O)-O groups on the

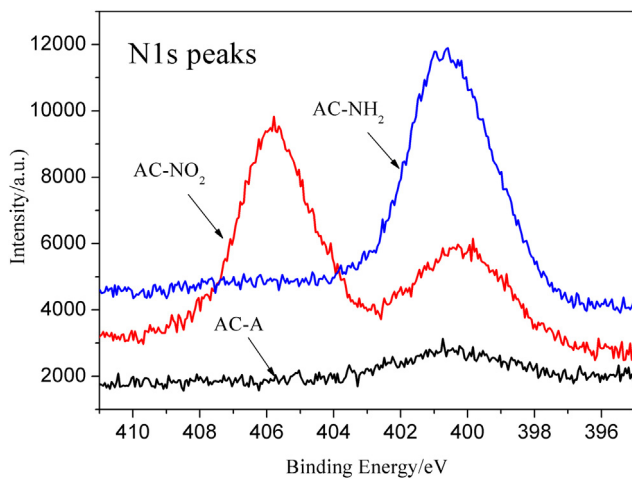


Fig. 3. N 1S peaks of different ACs.

surface greatly decreased after amination, consistent with the CO₂ profile in the TPD results.

As shown in Table 2, the content of nitrogen and oxygen on the AC surfaces both increased after surface modification. The existing forms of nitrogen were identified from their binding energies, as shown in Fig. 3. AC-NO₂ showed a strong peak at 405.8 eV, indicating the presence of nitrogen with a high oxidation state. The -NO₂ group was possibly modified on the surface, according to the literature [14,26]. Another component with a lower binding energy at 399.6 eV was also found and may correspond to the C-N-H bond [14,26]. After amination, the N-O peak completely disappeared, indicating the complete reduction of -NO₂ groups on the surface. The profile was completely identical with that reported by Masahiko Abe [14], because very similar method was adopted in the surface modification in the present work.

Surface chemical and physical adsorption analysis showed that the pore structure of AC-A was not destroyed during nitration and amination treatments. Acid oxygenated groups and -NO₂ groups were grafted onto the surface of AC-A after nitration, especially carboxylic groups. This grafting increased the acidity of the sample and deduced the number of basic groups on the surface. Oxygenated groups on AC-NO₂ were partially reduced by NaBH₄ in the amination step, whereas -NO₂ groups were completely reduced to -NH₂ groups. The pyrone and -NH₂ groups were responsible for the higher alkalinity of the sample.

3.2. Adsorption of OA on the surface modified AC samples

The adsorption of OA on different AC samples was investigated, and the results are shown in Fig. 4. The pK_{a1} and pK_{a2} of OA are 1.2 and 4.2, respectively. As a result, the OA existed in the solutions at pH 3 or 7 were mainly in the form of HOOC-COO⁻ and -OOC-COO⁻, respectively. In neutral solution, the AC-A and AC-NO₂ samples were both negatively charged ($pH_{pzc} < pH$). The electrostatic repulsion between -OOC-COO⁻ and the AC surface hindered adsorption, and only 1% and 0.7% of oxalic ions in bulk solution were adsorbed on AC-A and AC-NO₂, respectively. AC-NH₂ was electrically neutral in the solution with pH 7. Therefore, the adsorption of oxalic ions on AC-NH₂ was also weak and only 0.7% was adsorbed.

In the solution with pH 3, the oxalic ions mainly existed in the form of HCOO⁻. The AC-A and AC-NO₂ samples were less negatively charged in this solution. Approximately 4.7% of oxalic ions in bulk solution were adsorbed onto AC-A. The AC-NO₂ hardly adsorbed oxalic ions in this acid solution, because of the electrostatic repulsion and the dramatically decreased surface area.

Table 2
Elemental composition on the surfaces of different AC samples.

| Samples | Elemental composition (%) | | | O/C ($\times 100$) | N/C ($\times 100$) |
|--------------------|---------------------------|------|-----|----------------------|----------------------|
| | C | O | N | | |
| AC-A | 88.8 | 10.7 | 0.5 | 12.0 | 0.6 |
| AC-NO ₂ | 73.1 | 23.1 | 3.8 | 31.6 | 5.2 |
| AC-NH ₂ | 77.0 | 18.7 | 4.3 | 24.3 | 5.6 |

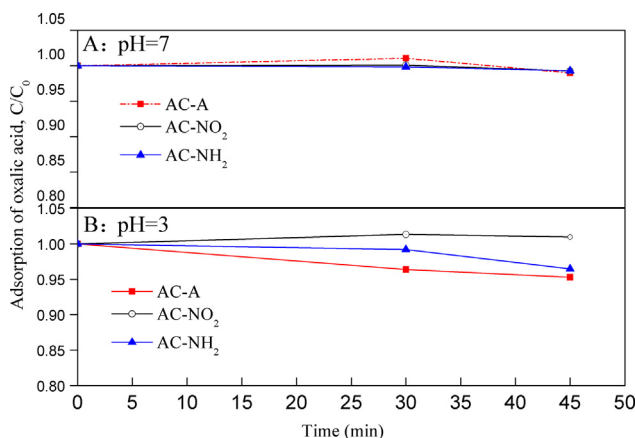


Fig. 4. Adsorption of oxalate on the different AC samples (A: pH = 7, B: pH = 3, C_0 = 50 mg/L, AC = 0.2 g/L).

The positive charge of AC-NH₂ enhanced the adsorption of oxalic ions because of increased electronic attraction, resulting in the adsorption of 3.5% of oxalic ions. The lower adsorption capacity and higher pH_{pzc} of AC-NH₂ compared with those of AC-A indicated that non-electrostatic adsorption may have also occurred during this adsorption process. Notably, although the adsorbed amount of oxalic ions at pH 3 was low, the concentration on the surface of AC was calculated to be extremely higher than that in bulk solution, and this will make sense in the surface catalytic reactions.

3.3. Ozonation and catalytic ozonation of OA

The ozonation and catalytic ozonation of OA at different pH values were investigated, and the results are shown in Fig. 5. Only 4% of OA was degraded in the solution at pH 3 during ozonation in 45 min, whereas the amount increased to 25.4% in neutral solution. This result was expected because OA directly reacted with ozone at a very low rate ($k_{O_3} \leq 0.04 M^{-1} s^{-1}$) [27], whereas •OH was significantly more reactive with OA at pH > 5 ($k_{\cdot OH} = 7.7 \times 10^6 M^{-1} s^{-1}$) [28]. Ozone self-decomposes to •OH in the presence of OH⁻. Thus, given the significantly larger amount of HO⁻ in neutral solution, higher amount of •OH was generated from ozone through chain reactions and resulted in the higher removal rate of OA.

When 0.2 g/L of the AC materials was added, a synergistic effect between ozone and the AC samples was observed, especially at pH 3. OA was much more easily removed in the acid solution with the O₃/AC system, and the removal rate increased to approximately 85%. AC-NO₂ and AC-NH₂ were both more active than AC-A, but the difference was not obvious. Apparently, AC samples also enhanced ozonation in neutral solution. The removal rates of OA on AC-NO₂, AC-NH₂ and AC-A were 53.6%, 42.4% and 38.7%, respectively. These values were all higher than the 25.4% during ozonation.

The activity of the AC-A sample was partially enhanced in the neutral and acidic solutions regardless of its acidity or basicity after surface modification. The AC-NH₂ became more basic and showed higher activities. This result was consistent with the generally accepted observation that basic groups favored catalytic ozonation in •OH oxidation. Apart from pyrone groups, the electron donating function of the —NH₂ group also increased the electron density of AC and enhanced the interaction between AC and molecular ozone. Meanwhile, the positively charged surface of AC-NH₂ also increased its adsorption of OA in the acidic solution.

The more acidic sample AC-NO₂ also showed higher activity than AC-A. Considering that the surface area of the AC samples did not increase after modification, this improvement may be due to the

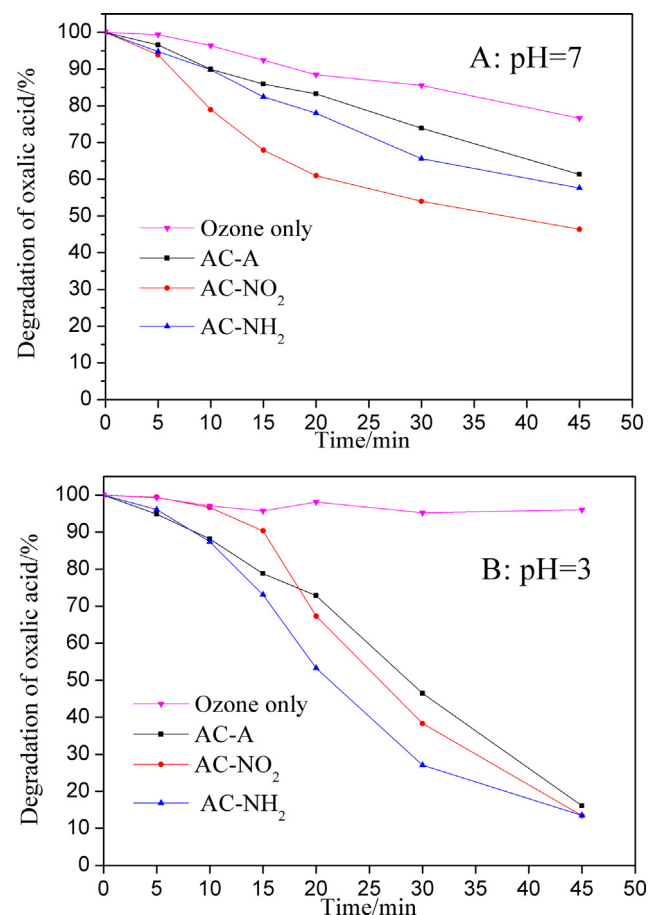


Fig. 5. Ozonation and catalytic ozonation of OA on AC samples (A: pH = 7, B: pH = 3, C_0 = 50 mg/L, AC = 0.2 g/L, O_3 = 50 mg/dm³).

change in surface chemical properties. Chedeville [12,13] similarly found that acid surface groups also improved the OA decomposition, i.e., •OH is generated and the removal of diethyl phthalate is enhanced. AC acts as a radical initiator, promoter and reaction support in such case.

Surface catalytic reaction and hydroxyl radical oxidation simultaneously occur in catalytic ozonation. The contribution of these reactions to the destruction of organics varied depending on the solution pH and surface properties of the catalyst [12]. In the AC/ozone system for OA and oxamic acid decomposition, Fabia [29] reported that AC and HNO₃ modified AC samples were both more active in pH 3 solution than in a neutral solution. The addition of *tert*-butanol (*t*-BA) did not inhibit the oxidation of organic compounds, and the oxidation mainly occurred on the AC surface [29]. Chedeville [12] also found a significant decrease in O₃/AC interaction at pH > 5, which might be due to the electrostatic repulsion between the species in solution and the AC surface. In the present study, the higher pH in the neutral solution also caused a lower O₃/AC interaction than that at pH 3, and slowed down the rate of ozone decomposition. In addition, the adsorption of OA on the AC materials at pH 3 also increased in this work, resulting in enhanced removal of OA though the surface catalytic reaction. By considering the contribution of hydroxyl radical oxidation, the rate constants of HO[•] with HOOC—COOH, HOOC—COO[−] and —OOC—COO[−] were $(1.0 \pm 0.1) \times 10^6$, $(3.2 \pm 0.1) \times 10^7$ and $(5.3 \pm 0.3) \times 10^6 M^{-1} s^{-1}$, respectively [30]. HO[•] mainly reacted with HOOC—COO[−] and —OOC—COO[−] and pH 3 and 7, respectively. The lower reaction rate of oxalic ions with HO[•] at pH 7 also accounted for its lower removal rate in the catalytic ozonation.

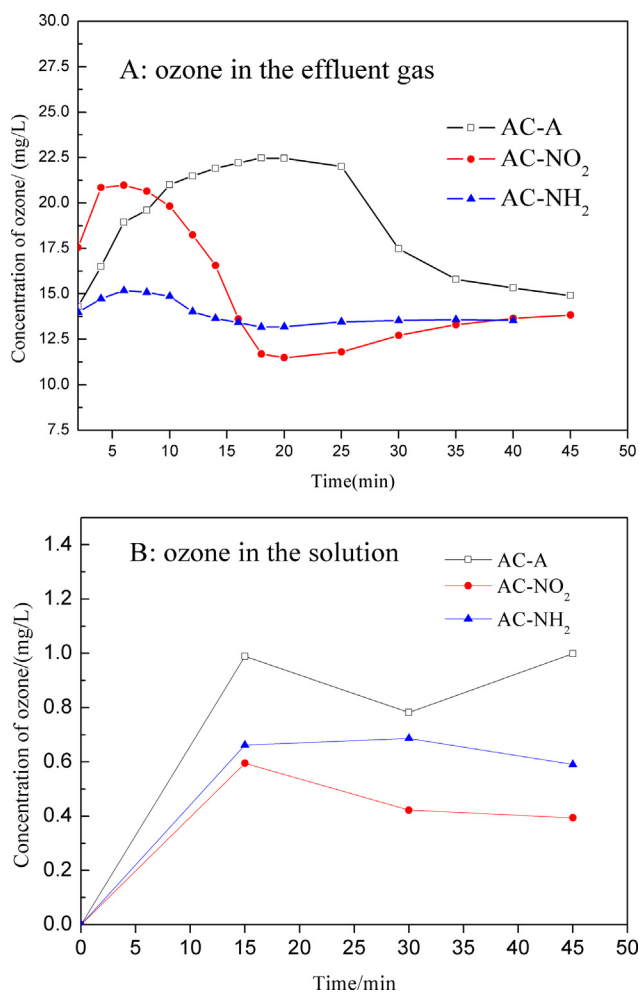


Fig. 6. Evolution of ozone in solution and in the effluent gas ($\text{pH} = 3$, $C_0 = 50 \text{ mg/L}$, $\text{AC} = 0.2 \text{ g/L}$).

Given the very low reaction rate of ozone with OA, only a trace amount of ozone was consumed in the system without a catalyst. The ozone concentration in the solution of pH 3 was about 9 mg/L, whereas that in the effluent gas rapidly reached 47 mg/dm³ and remained stable during ozonation of OA. When the AC samples were added as a heterogeneous catalyst, the ozone concentration in the solution and in the effluent gas both decreased. Fig. 6 shows the ozone concentration during catalytic ozonation of OA at pH 3. This result indicated that all AC samples were highly effective in catalyzing ozone decomposition. Furthermore, as shown in Fig. 6, ozone was rapidly consumed after 10 min in the system with the surface modified AC. This was consistent with the OA degradation curves in Fig. 5. The ability of AC-A to decompose ozone molecular was enhanced by surface modification, which is the main reason for their higher activity in OA degradation.

The concentration of inorganic carbon (IC) was monitored during OA degradation with AC-NO₂ and the results were shown in Fig. 7. IC originated from the dissolution of CO₂, and existed in the form of HCO₃⁻ in the solution with pH 4.0–8.3. The curves in Fig. 7 shows a significantly higher amount of HCO₃⁻ was presented in the neutral solution than in the acidic solution. An acidic solution favored the formation of CO₂ and H₂CO₃. Therefore, the generated CO₂ from OA oxidation in this semi-batch reactor system can be more easily obtained with an oxygen/ozone mixture in the acidic solution. This phenomenon can explain the lower IC concentration detected despite the rapid oxidation of OA in the acidic solution.

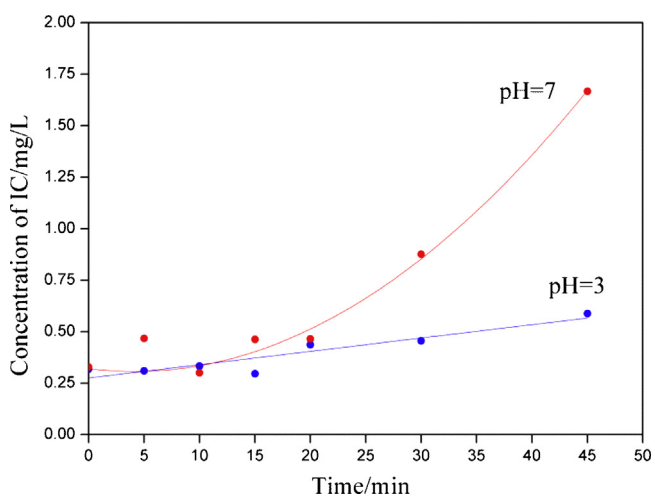


Fig. 7. Evolution of inorganic carbon (IC) during the catalytic ozonation of OA ($C_0 = 50 \text{ mg/L}$, $\text{AC} = 0.2 \text{ g/L}$).

Meanwhile, HCO₃⁻ is a strong scavenger of ·OH in solution because it quickly reacts with hydroxyl radical with a rate constant $k = 1.6 \times 10^7 \text{ M}^{-1} \text{ s}^{-1}$ [6]. For the OA oxidation involving ·OH, the higher concentration of HCO₃⁻ may slightly lower the OA removal rate in neutral solution. This phenomenon can be a supplemental explanation to the results in Fig. 5.

The mechanism of ·OH reaction and surface reaction were both reported in the AC-ozone reaction system. The adding of *t*-BA as an ·OH scavenger in the solution is an effective method to verify the main reaction mechanism. Fig. 8 shows that OA degradation was hindered by the addition of *t*-BA at pH 3 and 7. This result indicated that ·OH oxidation played an important role in OA oxidation.

The increase in the OA concentration during the reaction was interesting. The oxidation of *t*-BA did not generate OA; thus, AC was the only carbon source that produced short chain carboxylic acids. These short chain carboxylic acids may originate from the partial oxidation of functional groups on the AC surface. In a free organic ozonation process, Beltrán [31] found that the TOC and UV₂₅₄ of the solution gradually increased because of the strong interaction between PAC and ozone. Furthermore, the TOC also increased in the catalytic ozonation of sulfamethoxazole oxidation intermediates with preozonated PAC as catalyst [31]. This result can explain the similar phenomenon observed in our experiment. This strong interaction between molecular ozone and the AC surface also indicated strong adsorption of AC onto the ozone molecule, which benefited surface catalytic oxidation.

The ozone concentrations in the solution and effluent gas during OA decomposition were also recorded. The concentrations in the pH 3 and 7 solutions both increased after the addition of *t*-BA. A similar result was observed in the effluent gas. These findings indicated that a smaller amount of ozone was decomposed in this process. ·OH rapidly reacted with *t*-BA ($k = 5 \times 10^8 \text{ M}^{-1} \text{ s}^{-1}$) [32]. In addition, a number of inert products were produced and subsequently terminated the chain reaction of ozone decomposition. The removal rate of OA and the degradation rate of ozone both decreased in this case, thereby indicating the vital role of ·OH oxidation in OA degradation [33].

Nitration modification was a combined result of nitric acid and acetic anhydride. Acid oxygenated groups and —NO₂ group were simultaneously modified during nitration treatment. These groups exhibited a positive effect on the catalytic ozonation of OA. Deprotonated acid functional groups can interact with ozone to generate O₂·⁻ and O₃·⁻, which function as radical promoters in chain reactions to generate ·OH [13]. Valdés [34] found that

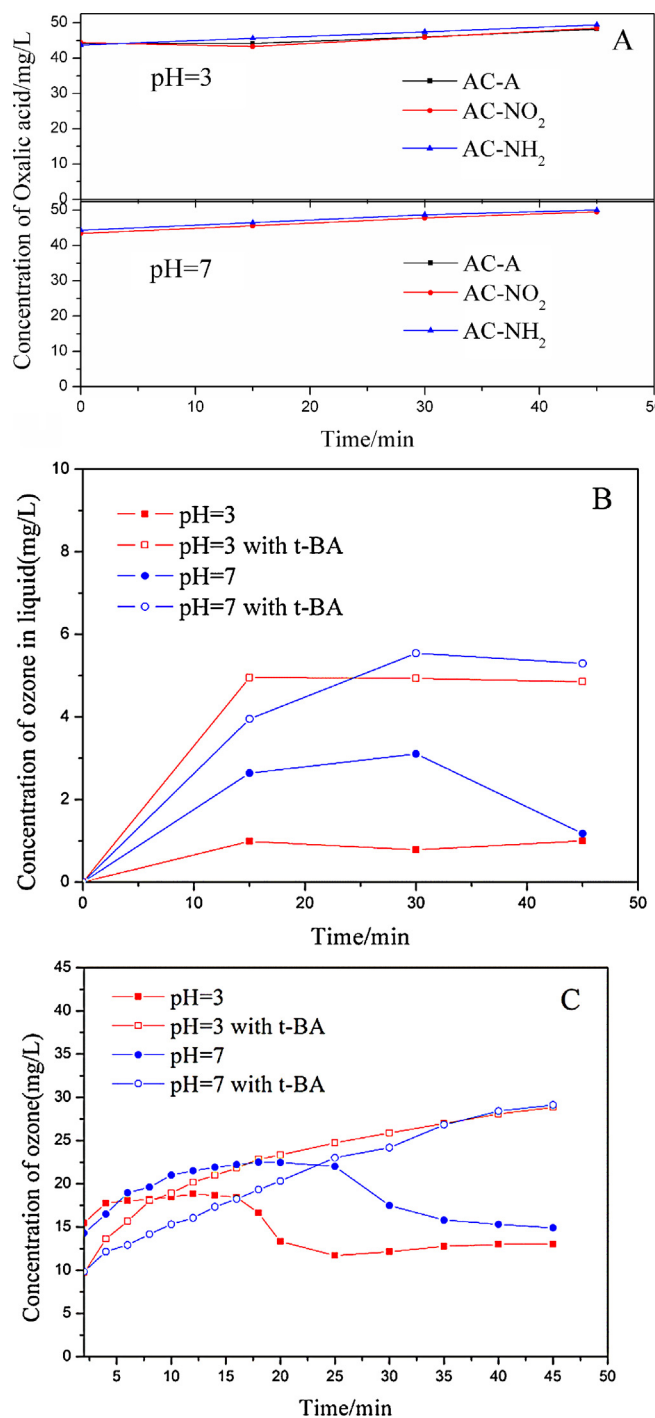


Fig. 8. Catalytic ozonation of OA on AC-NO₂ with *tert*-butanol (t-BA) in solution (A), ozone concentrations in the solution (B) and in the effluent gas (C), $C_0 = 50 \text{ mg/L}$, AC = 0.2 g/L, $C_{\text{t-BA}} = 2 \text{ mM}$.

dissociated acid groups on an AC sample were responsible for the increased ozone decomposition rate at $\text{pH} > \text{pH}_{\text{pzc}}$. These results are consistent with those obtained in the present work, i.e., nitrated samples became more acidic and had higher activities toward OA removal than the AC-A sample. It was very hard to experimentally evaluate the function of $-\text{NO}_2$ group in this work. Because concentrated nitric acid is highly oxidative and it was difficult to modify $-\text{NO}_2$ group alone on the AC surface or in nitric acid, or in a mixed solution with acetic anhydride. As an electron attracting group, $-\text{NO}_2$ lowers the electron density of the connected aromatic rings or the carbon atoms on the surface of AC. The lower electron

density does not benefit catalytic ozonation. Accordingly, the blocking effect of $-\text{NO}_2$ on catalytic ozonation and the higher activities of the AC-NO₂ sample suggested that acid oxygenated groups played a positive role in the catalytic ozonation of OA.

4. Conclusions

In the current study, the activity of a commercial AC in the catalytic ozonation of OA was enhanced after nitration or amination modification. The micropores of AC were not destroyed in these processes. The entrance of micropores was largely occupied by oxygenated groups in the nitration treatment. Meanwhile, the external surface area only slightly decreased during amination. pH_{pzc} values and Boehm titration results showed that the acid washed AC sample became more acidic after nitration, whereas its basicity increased after amination. TPD and XPS analysis revealed that a large amount of acid oxygenated groups and $-\text{NO}_2$ groups were grafted onto the AC surface during nitration. In the amination step, the oxygenated groups were partly reduced while $-\text{NO}_2$ groups were completely reduced. The basicity and electron donating effect of the $-\text{NH}_2$ group increased the activity of AC-NH₂ catalyst. Although the electron-withdrawing effect of the $-\text{NO}_2$ group exerted a negative effect on catalytic ozonation, nitrated AC materials showed enhanced activities in OA removal. Combing the textural analysis of the nitrated AC sample, it was confirmed that the acid oxygenated surface groups were benefit to catalytic ozonation. The increase in AC activity after nitration indicated that nitration is an effective method to improve the performance of ACs in catalytic ozonation.

Acknowledgements

The financial support from National Natural Science Foundation of China (21207133), the National Key Technology R&D Program (2011BAC06B09) and Visiting Professorships of Chinese Academy of Sciences for Senior International Scientists (2009G2-28) are greatly appreciated. This work was partially supported by Brook Byer Institute for Sustainable Systems, the Hightower Chair and Georgia Research Alliance. We also thank the anonymous reviewers for their very valuable comments to improve this work.

References

- [1] A.H. Lv, C.H. Hu, Y.L. Nie, J.Q. Qu, *Applied Catalysis B: Environmental* 100 (2010) 62–67.
- [2] J. Nawrocka, B. Kasprzyk-Hordern, *Applied Catalysis B: Environmental* 99 (2010) 27–42.
- [3] P.M. Alvarez, F.J. Beltrán, F.J. Masa, J.P. Pocostales, *Applied Catalysis B: Environmental* 92 (2009) 393–400.
- [4] J.C. Crittenden, S.M. Hu, D.W. Hand, S.A. Green, *Water Research* 33 (1999) 2315–2328.
- [5] M. Daisuke, W.H. Song, J. Crittenden, *Environmental Science & Technology* 45 (2011) 6057–6065.
- [6] B. Kasprzyk-Hordern, M. Ziolk, J. Nawrocki, *Applied Catalysis B: Environmental* 46 (2003) 639–669.
- [7] J. Rivera-Utrilla, M. Sánchez-Polo, V. Gómez-Serrano, P.M. Álvarez, M.C.M. Alvim-Ferraz, J.M. Dias, *Journal of Hazardous Materials* 187 (2011) 1–23.
- [8] M. Sánchez-Polo, U. von Gunten, J. Rivera-Utrilla, *Water Research* 39 (2005) 3189–3198.
- [9] Z.Q. Liu, J. Ma, Y.H. Cui, L. Zhao, B.P. Zhang, *Separation and Purification Technology* 78 (2011) 147–153.
- [10] P.C.C. Faria, J.J.M. Órfão, M.F.R. Pereira, *Industrial and Engineering Chemistry Research* 45 (2006) 2715–2721.
- [11] P.M. Álvarez, J.F. García-Araya, F.J. Beltrán, I. Giráldez, J. Jaramillo, V. Gómez-Serrano, *Carbon* 44 (2006) 3102–3112.
- [12] H. Dehouli, O. Chedeville, B. Cagnon, V. Caqueret, C. Porte, *Desalination* 254 (2010) 12–16.
- [13] T.F. de Oliveira, O. Chedeville, H. Fauduet, B. Cagnon, *Desalination* 276 (2011) 359–365.
- [14] M. Abe, K. Kawashima, K. Kozawa, *Langmuir* 16 (2000) 5059–5063.
- [15] M.A. Ferro-García, J. Rivera-Utrilla, I. Bautista-Toledo, C. Moreno-Castilla, *Langmuir* 14 (1998) 1880–1886.
- [16] P. Chingombe, B. Saha, R.J. Wakeman, *Carbon* 43 (2005) 3132–3143.

- [17] P. Chingombe, B. Saha, R.J. Wakeman, *Journal of Colloid and Interface Science* 302 (2006) 408–416.
- [18] C.O. Ania, J.B. Parra, J.J. Pis, *Fuel Processing Technology* 79 (2002) 265–271.
- [19] C. Moreno-Castilla, M.A. Ferro-Garcia, J.P. Joly, I. Bautista-Toledo, F. Carrasco-Marin, J. Rivera-Utrilla, *Langmuir* 11 (1995) 4386–4392.
- [20] I. Bautista-Toledo, J. Rivera-Utrilla, M.A. Ferro-Garcia, C. Moreno-Castilla, *Carbon* 32 (1994) 93–100.
- [21] C.M. Ghimbeu, R. Gadiou, J. Dentzer, D. Schwartz, C. Vix-Guterl, *Langmuir* 26 (2010) 18824–18833.
- [22] O.W. Fritz, K.J. Huttinger, *Carbon* 31 (1993) 923–930.
- [23] H. Valdés, M. Sánchez-Polo, J. Rivera-Utrilla, C.A. Zaror, *Langmuir* 18 (2002) 2111–2116.
- [24] P. Brender, R. Gadiou, J.C. Rietsch, P. Fioux, J. Dentzer, A. Ponche, C. Vix-Guterl, *Analytical Chemistry* 84 (2012) 2147–2153.
- [25] M.C. Yang, T.S. Yang, M.S. Wong, *Thin Solid Films* 1 (2004) 469–470.
- [26] E. Bekyarova, M.E. Itkis, P. Ramesh, C. Berger, M. Sprinkle, W.A. de Heer, R.C. Haddon, *Journal of the American Chemical Society* 131 (2009) 1336–1337.
- [27] G.V. Buxton, C.L. Greenstock, W.P. Helman, A.B. Ross, *Journal of Physical and Chemical Reference Data* 17 (1988) 513–886.
- [28] J. Hoigné, h. Bader, *Water Res* 17 (1983) 185–194.
- [29] P.C.C. Faria, J.J.M. Órfão, M.F.R. Pereira, *Applied Catalysis B: Environmental* 79 (2008) 237–243.
- [30] N. Getoff, F. Schwörer, V.M. Markovic, K. Sehested, S.O. Nielsen, *Journal of Physical Chemistry* 75 (1971) 749–755.
- [31] J.P. Pocostales, P.M. Alvarez, F.J. Beltrán, *Chemical Engineering Journal* 164 (2010) 70–76.
- [32] B. Langlais, D.A. Reckhow, D.R. Brink (Eds.), *Ozone in Water Treatment: Application, Engineering*, Lewis Publishers, Chelsea, MI, USA, 1991.
- [33] J. Ma, J.D. Nigel, Graham, *Water Research* 15 (2000) 3822–3828.
- [34] H. Valdés, C.A. Zaror, *Chemosphere* 65 (2006) 1131–1136.